

ChemComm

Accepted Manuscript



This is an *Accepted Manuscript*, which has been through the Royal Society of Chemistry peer review process and has been accepted for publication.

Accepted Manuscripts are published online shortly after acceptance, before technical editing, formatting and proof reading. Using this free service, authors can make their results available to the community, in citable form, before we publish the edited article. We will replace this *Accepted Manuscript* with the edited and formatted *Advance Article* as soon as it is available.

You can find more information about *Accepted Manuscripts* in the [Information for Authors](#).

Please note that technical editing may introduce minor changes to the text and/or graphics, which may alter content. The journal's standard [Terms & Conditions](#) and the [Ethical guidelines](#) still apply. In no event shall the Royal Society of Chemistry be held responsible for any errors or omissions in this *Accepted Manuscript* or any consequences arising from the use of any information it contains.

COMMUNICATION

Mitochondrion Targeting Fluorescent Probe for Imaging of Intracellular Superoxide Radical

Fang Si,^{a,b} Yang Liu,^c Kelu Yan^b and Wenwan Zhong^{a,c*}

Received 00th January 2012,
Accepted 00th January 2012

DOI: 10.1039/x0xx00000x

www.rsc.org/

An amine-reactive fluorogenic molecule specifically turned on by superoxide radicals ($O_2^{\cdot-}$) was synthesized and coupled to a mitochondrial (MT) targeting peptide. The obtained probe showed superior uptake and MT targeting capabilities; and successfully detected the change of $O_2^{\cdot-}$ levels in cells treated by chemical stimuli or single-walled carbon nanotubes.

Biological systems continuously produce free radicals via a wide range of physiological processes. The radicals can act as secondary messengers and control diverse activities like host defense, inflammation, and cellular signalling.¹⁻⁴ The levels of radicals are tightly controlled by a series of antioxidants and enzymes.^{5,6} If the balance is broken due to malfunctioning of the antioxidant protection systems, damages including aging and pathological conditions like cancer, cardiovascular, inflammatory and degenerative diseases, could occur.^{3,4,7,8} Still, not enough is known about the mechanisms of oxidant and antioxidant action so that effective interventions can be designed, calling for more powerful methodologies to be developed for detecting oxidant production specifically and quantitatively.

Generally produced from oxygen reduction by electrons leaked out from the mitochondrial respiratory chains, superoxide radical ($O_2^{\cdot-}$) is the common source of most of the reactive oxygen or nitrogen species (ROS or RNS) found in cells.^{7,9-11} It can go through dismutation and form H_2O_2 ,¹² or be oxidized by NO and generate ONOO⁻.^{6,9,13,14} These products then continue to react and produce a series of ROS and RNS. Such an essential role makes it imperative to assess $O_2^{\cdot-}$ generation in mechanistic studies on oxidative damage and antioxidant protection.^{10,11}

Current tools for $O_2^{\cdot-}$ assessment often fall in three categories: detection of the unpaired electron by electron spin resonance (EPR); electrochemical sensors based on its redox property; and optical methods that permits high-throughput screening and imaging in live cells and animals. They can effectively detect the presence of superoxide radicals, but still have limitations. For example, spin traps have been developed to detect superoxide and hydroxyl radical by EPR, but they are only suitable for measurement of extracellular radicals.¹⁵⁻¹⁹ Similarly, electrochemical sensors utilizing immobilized enzymes, nanoparticles, or microelectrodes, have been fabricated for detection of superoxide released by cells or in solutions.²⁰⁻²⁴ Electrodes with immobilized enzymes can provide

good specificity but are complicated and delicate to fabricate.²¹⁻²³ Because of their measurement simplicity and capability to enable *in vitro* and even *in vivo* imaging, optical methods have been widely used, taking advantages of various fluorescence and chemiluminescent probes.^{25,26} They offer good sensitivity, either by the dye itself²⁷ or by nanoparticle-assisted signal enhancement;²⁸ and can dynamically image $O_2^{\cdot-}$ fluctuation using the two-photon technology.²⁹ However, specificity is a big concern. The cyanine-based sensors simultaneously detect other ROS like hydroxyl radical together with superoxide.^{30,31} Hydroethidine (HE), the most common fluorescent sensor for $O_2^{\cdot-}$, can be oxidized by other intracellular processes involving peroxidase and cytochromes to more than one red fluorescence products.^{32,33} Specificity of the HE-based fluorescence assay can be enhanced by HPLC separation of the multiple products,^{34,35} or by using two different excitation wavelengths.³³

Similar cross-reaction problems could exist for other fluorescent probes that sense superoxide radicals based on redox reactions.

Besides high sensitivity and specificity, imaging probes should target specific organelles, because superoxide radicals are typically generated in mitochondria via respiration, in phagosomes by NADPH oxidase for defense of invading pathogens, or in endoplasmic reticulum during

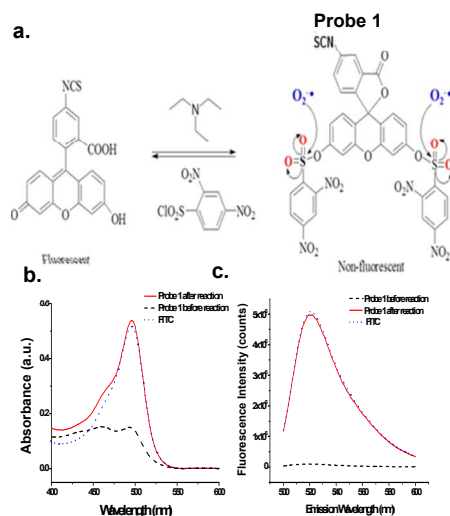
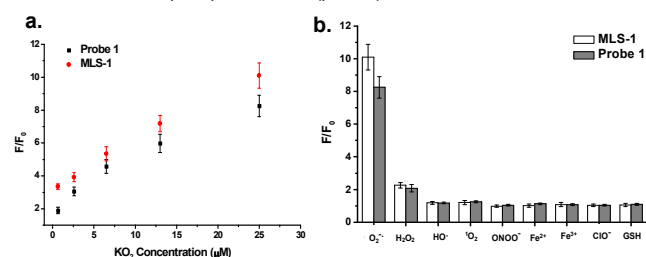


Figure 1. a) Synthesis process of probe 1. The sulfonyl groups could be nucleophilic substituted by $O_2^{\cdot-}$ to emit strong fluorescence. The b) absorption and c) fluorescence emission ($\lambda_{ex}=495$ nm) spectra of $32 \mu M$ 1 before and after reaction with $100 \mu M$ KO_2 in 50 mM phosphate buffer (pH 7.4). The spectra of FITC were also displayed.

process of protein folding.¹¹ Their anionic nature makes them impermeable through the organelle membranes and they are converted at their production sites by enzymes or other processes. Monitoring their production and conversion for mechanistic study thus requires probes that can specifically locate at the production sites to gain more information.

A group of fluorescent probes that detect superoxide via a

Figure 2. a) Fluorescence change for 10 μM probe 1 and MLS-1 after 10 min. reaction with 0, 0.65, 2.6, 6.5, 13, and 25 μM KO_2 in 50 mM phosphate buffer (pH 7.4). b) Probe 1 and MLS-1 showed large fluorescence change after reaction with 25 μM O_2^- , but negligible change with 50 μM H_2O_2 , NaONO , HO^\cdot , and $^1\text{O}_2$, or with 100 μM GSH , NaClO , FeSO_4 , and FeCl_3 . All data were obtained in 50 mM phosphate buffer (pH 7.4) with EX/EM at 494/520nm.



nonredox mechanism have been reported by Itoh *et al.*^{36,37} Superoxide reacts with this group of bis(2,4-dinitrobenzenesulfonyl) fluorescein molecules as a nucleophile, instead of as a reductant. The reaction causes the cleavage of the benzenesulfonyl groups, turning on the fluorescence of fluorescein. Similar reaction mechanism was also employed to design the turn-on O_2^- sensor molecule, bis(diphenylphosphinyl) fluorescein.³⁸ However, localized detection of endogenous O_2^- has not been demonstrated with such dyes. Following the same synthetic route discovered by the Itoh group, we prepared the bi-substituted Bis(2,4-dinitrobenzenesulfonyl) fluorescein isothiocyanate (**1**) (Figure 1a). The isothiocyanate (-SCN) group is not only readily reactive to free amines that enables easy conjugation to biological molecules, but also enhances the probe's specificity to O_2^- . Conjugated to the mitochondrial locating

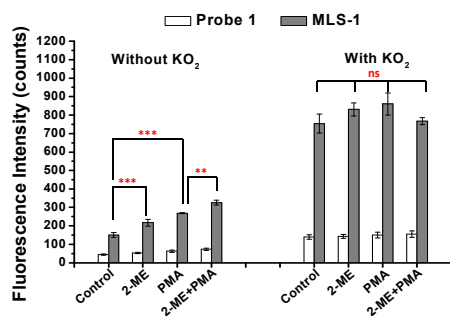


Figure 3. Responses of probe 1 and MLS-1 to changes in O_2^- content in Raw 264.7 macrophages induced by PMA and 2-ME. The two stimulators were used either individually or in combination. Their uptake by the cells was evaluated after 10-min reaction with 25 μM KO_2 . Five μM of probe 1 or MLS-1 were used for cell incubation and the cell lysate was diluted by 60 μL 50 mM phosphate at pH 7.4. Note: *** = $p < 0.005$; ** = $p < 0.01$, * = $p < 0.05$, ns = no significant difference.

walled carbon nanotubes (SWCNTs).

The reaction scheme is shown in Figure 1a. In brief, fluorescein isothiocyanate (FITC) reacted with 2,4-dinitrobenzenesulfonyl chloride in dichloromethane (DCM) under the catalysis of trimethylamine. The obtained product was characterized by ^1H -NMR (Figure S1a, ESI[†]) and MS (Figure S1b, ESI[†]) to confirm the high purity of the bi-substituted compound. This is important

because the mono-substituted product is prone to hydrolysis and is reactive to thiol-containing compounds, both able to turn on its fluorescence.^{36, 37} The bi-substituted compound, probe 1, absorbed poorly in between 450 to 520 nm (Figure 1b), and exhibited negligible fluorescence at λ_{em} of 520 nm when excited at 494 nm (Figure 1c). After reaction with KO_2 , the superoxide generator, the absorption and fluorescence emission spectra were similar to those from FITC at the same concentration (Fig. 1b & c). The probe reacts with O_2^- very rapidly, reaching the plateau in less than 10 minutes after being mixed with KO_2 (Figure S2a, ESI[†]). The resulted fluorescence linearly increased with KO_2 concentration. As low as 0.65 μM KO_2 could be detected using 10 μM probe 1 (Figure S2b, ESI[†]). The signal levelled off once all the probes were consumed with KO_2 higher than 25 μM (Fig. S2a, ESI[†]). This result suggests that, two O_2^- were needed to remove the two dinitrobenzenesulfonyl groups and convert one probe 1 molecule back to FITC.

Probe 1 has no targeting capability for mitochondria (MT). Therefore, we conjugated it to one of the MLS targeting peptide at the N-terminal via the reaction between -SCN and -NH₂. This peptide is the N-terminal portion of one of the endogenous nuclear-encoded MT proteins.³⁹ This portion is responsible for transportation of such proteins into MT, via its interaction with the translocator inner membrane/translocator outer membrane protein complex. The selected peptide contains one lysine residue at the C-terminal that could also be labelled. HPLC analysis showed all free probe 1 had been conjugated with the peptide (Figure S3, ESI[†]).

The MLS-1 conjugate displayed comparable fold change to probe 1 in fluorescence intensity upon reaction with KO_2 (Figure 2a). The fluorescent product of probe 1 is fluorescein, the fluorescence of which is very sensitive to pH.⁴³ We observed only background fluorescence from probe 1 or MLS-1 after reaction KO_2 if the solution pH was at 5.8. The fluorescence increased dramatically at pH 6.5, reaching the maximum at 8 and being stable up to pH 10 (Figure S4, ESI[†]). This result points out that our probe is suitable for superoxide measurement in cytosol (pH 7.0-7.5), endoplasmic reticulum (pH ~7.2), Golgi apparatus (pH ~ 6.6), and most importantly mitochondrion (7.9-8.0).^{44, 45} But it cannot be used to image superoxide in the acidic organelles like endosome and lysosome. The pH sensitivity of probe 1 also highlights the necessity of using the MLS peptide to deliver the probe to the right intracellular location. The MLS-1 conjugate maintained good selectivity to superoxide radicals over other common interferences like H_2O_2 , $\cdot\text{OH}$, ONOO^\cdot , ClO^\cdot , and the iron ions (Figure 2b). Both probe-1 and MLS-1 showed no reactivity to GSH, a potential interfering compound present at substantial levels in cells.^{36, 42}

We tested the cellular uptake of MLS-1 and its capability to detect O_2^- change in cells. The Raw 264.7 macrophages (grown in a 24-well microtiter plate at an approximate density of 1×10^4 /well) were treated sequentially with 20 $\mu\text{g}/\text{ml}$ 2-ME for 4 hrs, 5 μM probe 1 or MLS-1 for 40min, and 5 $\mu\text{g}/\text{mL}$ PMA for 30 min. The culture medium was refreshed after incubation with the probes. Thereafter, the cells were washed with $1 \times \text{PBS}$ for 3 times to remove any residual chemicals not entering the cells, and then incubated with CellLytic™ M, the mammalian cell lysis/extraction reagent from Sigma, for 15 min on a shaker. Upon cell lysis, an aliquot 60 μL of 50 mM phosphate buffer at pH 7.4 was added to each well to suspend the released probe 1 or MLS-1 before fluorescence measurement in Victor 2 Microplate Reader (Perkin Elmer). The results were shown on the left panel labelled as “without KO_2 ” in Figure 3. The control sample was not treated with either 2-ME or PMA, showing the base level of O_2^- in cells. Some of the O_2^- may have been generated during cell lysis. Nevertheless, the MLS-1 detected a significantly higher level of O_2^- in the cells treated by 2-ME compared to the

control cells. This chemical is an inhibitor of superoxide dismutase (SOD), the dominant working machine in converting superoxide into H_2O_2 . Deactivating SOD caused accumulation of $\text{O}_2^{\cdot-}$ in cells and thus a higher fluorescence signal was observed from MLS-1. The paired t-test confirmed that the fluorescence signals from MLS-1 in control cells and in cells treated with 2-ME were significantly different at the confidence level of 95% with a p value smaller than 0.005 (n = 3).

Similarly, the $\text{O}_2^{\cdot-}$ content was significantly higher in cells treated by PMA, a chemical known to stimulate superoxide generation, with a p value smaller than 0.01. The combined effect of 2-ME and PMA generated the highest level of $\text{O}_2^{\cdot-}$ in cells.

Using probe 1, the overall fluorescence was very low, although noticeable increase in fluorescence was found in cells treated with PMA or with PMA+2-ME. The weak signal was due to its low cellular uptake. Cellular uptake was evaluated by adding 10 μM KO_2 to react with all probe 1 or MLS-1 used in cell treatment, after the aforementioned fluorescence measurement was finished. Such a KO_2 concentration is sufficient to convert all probe 1 molecules to fluorescein in cell lysate. The resulted fluorescence was shown in

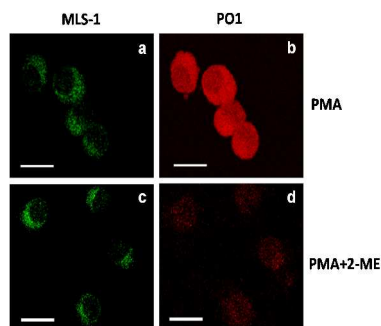


Figure 5. Confocal fluorescence images of MLS-1 co-stained with PO1 in RAW 264.7 Macrophages. The green ($\lambda_{\text{ex}} = 488 \text{ nm}$; $\lambda_{\text{em}} = 500\text{-}535 \text{ nm}$) (a and c) and red ($\lambda_{\text{ex}} = 543 \text{ nm}$; $\lambda_{\text{em}} = 555\text{-}700 \text{ nm}$) (b and d) channels were collected in cells stimulated by PMA (a-b) alone or in combination with 2-ME (c-d). Scale bar = 20 μm .

the cell culture medium and thus removal of probe 1 during the washing step, we reacted the -SCN group with a small amine, methylamine, and tested the cellular uptake of the product. No improvement was observed and the overall uptake of the methylamine labelled probe 1 was still much lower than that of the

MLS-1 (Figure S5, ESI \dagger). This means the low uptake was the result of the fluorophore structure.

It is also important that the intracellular sensor does not generate harmful effect to cells. Thus, we treated the Raw 264.7 macrophages at various probe 1 and MLS-1 concentrations (1, 2.5, 5, and 10 μM), and tested cell viability using the MTT assay. After 6, 12, or 24 hrs incubation with MLS-1, the viability of the Raw 264.7 cells was not affected (Figure S6, ESI \dagger). Probe 1 at 10 μM reduced the cell viability to around 90% after 24 hrs incubation. While the superior safety of MLS-1 permits its usage as an intracellular sensor for $\text{O}_2^{\cdot-}$, the MLS peptide should locate the probe right at MT, so that localized monitoring of radical production can be achieved. Dye localization was confirmed by co-staining the cells with both the superoxide sensor and MitotrackerTM Red (Invitrogen). Since probe 1 or MLS-1 was not fluorescent before reacting with superoxide, the cells were also treated by 2-ME and PMA to stimulate radical generation so that MT localization could be observed clearly. The procedure was similar to the cell uptake experiment, except that the dye was mixed with Mitotracker Red before added to the cells. After all treatments, the cells were washed and subsequently fixed with 4% formaldehyde at 37 $^{\circ}\text{C}$ for 15 min before fluorescence observation by Leica SP5 Inverted Confocal Microscope (Leica Microsystems, Inc.). Figure 4 showed the fluorescence images from MLS-1 (green) and Mitotracker (red), respectively. Both the green and red fluorescence were found in the cytosol around the nucleus, which was completely dark without being stained; and the overlaid images confirmed the co-localization of both MLS-1 and Mitotracker Red. On contrary, probe 1 was found at other places without red fluorescence, and even within the nucleus (Figure S7, ESI \dagger). Agreeing with the cell lysis experiments, the confocal images clearly showed the enhanced green fluorescence while both PMA and 2-ME were used to stimulate the cells, compared to the control cells and to those treated only with 2-ME, under the same light acquisition settings.

Superoxide radicals have short life time because they will be converted to other ROS/RNS by enzymes. One of the main conversion routes is by SOD and the process forms H_2O_2 . To demonstrate that our probe is suitable to image the dynamic change of superoxide radicals, we imaged this conversion process by using both our probe and the red H_2O_2 sensor from TrocristTM Bioscience, peroxy orange 1 (PO1).⁴⁶ PO1 can be excited at 543 nm, and emits between 555 and 700 nm. Thus, we can image the fluorescence resulted from both $\text{O}_2^{\cdot-}$ and H_2O_2 simultaneously using PO1 and MLS-1. Both dyes were lit up when the cells were incubated with PMA (Figure 5; fluorescence from PO1 was represented in red). However, in the cells treated by both PMA and 2-ME, the fluorescence from PO1 was much weaker, because 2-ME impeded with the conversion of $\text{O}_2^{\cdot-}$ to H_2O_2 , while the green fluorescence from MLS-1 remained intense and was accumulated at specific sites where the MT located. This result also serves as a convincing support for our probe's high selectivity for superoxide radicals over H_2O_2 .

Using this superoxide-specific and MT-targeting conjugate, MLS-1, we studied the oxidative stress induced by

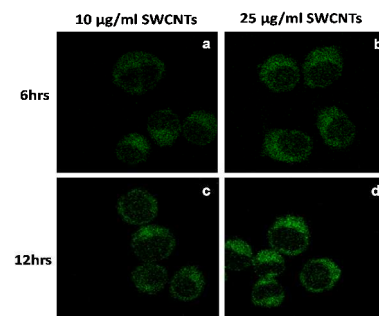


Figure 6. Confocal fluorescence images of MLS-1 in RAW 264.7 Macrophages stimulated by SWCNTs for 6 (a-b) or 12 hrs (c-d), acquired in the green ($\lambda_{\text{ex}} = 488 \text{ nm}$; $\lambda_{\text{em}} = 500\text{-}535 \text{ nm}$) Scale bar = 20 μm .

invasion of single-walled carbon nanotubes (SWCNTs). MTT assay showed that incubating the Raw 264.7 macrophages with the carboxylated SWCNTs at concentration of 5, 10, 25, and 50 $\mu\text{g}/\text{mL}$ caused significant cell death (Figure S6, ESI†): lower than 70% viability was observed with the highest SWCNT concentration during 6 hrs incubation, and also with the 3 higher SWCNT concentrations after 12 or 24 hrs incubation. Fluorescence imaging using MLS-1 for incubation with 10 and 25 $\mu\text{g}/\text{mL}$ SWCNTs for 6 and 12 hrs were shown in Figure 6 (the images for other concentrations and incubation durations shown in Figure S8, ESI†). The green fluorescence from MLS-1 in MT increased gradually with the increase of SWCNT concentration and/or incubation duration. This result points out that SWCNT invasion enhanced superoxide production, which was rapidly converted to H_2O_2 (confirmed by PO1 staining; data not shown). Finally the elevated oxidative stress resulted in cell death.

The MLS-1 was also applied to image superoxide production in epithelial cells (Hela ATCC[®] CCL-2TM) (Figure S9, ESI†). Similar to the results from macrophages, low toxicity and good targeting capability were observed, and the changes in superoxide levels caused by chemicals were clearly detected, demonstrating its applicability to diverse cell types.

Conclusions

We have generated a fluorescence probe that has excellent specificity at detecting superoxide radicals, and can specifically target MT without producing harmful effects. It can be used to monitor the dynamic change of superoxide radical levels in cells, as demonstrated in the present study using both small chemicals and carbon nanomaterials. The amine reactivity of probe **1** also permits labelling with other biomolecules such as antibodies or molecules targeting other organelles to detect generation of superoxide radicals at other locations inside the cells. Considering the central role of superoxide radical in cellular production of ROS/RNS, our probe can be a useful tool in deciphering its functions in cell signalling and host defense. Coupling with dyes specific for other ROS/RNS, it can also help with screening for chemicals that could damage enzymes involving in the conversion processes.

This work was supported by NSF CAREER CHE #1057113 to W. Zhong and S. Fang was sponsored by the China Scholarship Council. The authors were also thankful to the support from the City of Hope Biomedical Research Initiative.

Notes and references

^a Department of Chemistry, ^c Environmental Toxicology Program, University of California, Riverside, USA 92521; ^b College of Chemistry, Chemical and Biological Engineering, Donghua University, Shanghai, P. R. China 201620.

* Corresponding author: wenzhong@ucr.edu; 001-951-827-4925 (Tel); 001-951-827-4732 (FAX).

† Electronic Supplementary Information (ESI) available: experimental procedures, NMR and MS results, reaction rate investigation, detection calibration curve for probe **1** only, HPLC result to demonstrate purity of MLS-1, comparison of response with excess $\text{O}_2\cdot^-$ between **1** and MLS-1 in solution, cell viability when incubated with probe **1**, MLS-1, and SWCNTs, imaging results for probe **1** intracellular location, images from MLS-1 to test SWCNT-induced generation of superoxide, and all results obtained in HeLa cells. See DOI: 10.1039/c000000x/

- 1 T. Akaike, *Rev. Med. Virol.* 2001, **11**, 87.
- 2 I. Bokkon, *Curr. Neuropharmacol.* 2012, **10**, 287.
- 3 P. C. Goswami and K. K. Singh, *Oxidative Stress, Disease Cancer* 2006, 705.
- 4 M. Majzunova, I. Dovinova, M. Barancik and J. Y. H. Chan, *J. Biomed. Sci.* 2013, **20**, 69.
- 5 M. G. Bonini and A. B. Malik, *Cell Res.* 2014, **24**, 908.
- 6 M. Inoue, E. F. Sato, A.-M. Park, M. Nishikawa, E. Kasahara, M. Miyoshi, A. Ochi and K. Utsumi, *Free Rad. Res.* 2000, **33**, 757.

- 7 A. W. Linnane, M. Kios and L. Vitetta, *Mitochondrion* 2007, **7**, 1.
- 8 T. Takeuchi, M. Nakajima and K. Morimoto, *Carcinogenesis* 1996, **17**, 1543.
- 9 I. B. Afanas'ev, *Mol. Biotechnol.* 2007, **37**, 2.
- 10 C. C. Winterbourn, *Free Rad. Biol. Med.* 1993, **14**, 85.
- 11 C. C. Winterbourn, *Nat. Chem. Biol.* 2008, **4**, 278.
- 12 I. A. Abreu and D. E. Cabelli, *Biochim. Biophys. Acta* 2010, **1804**, 263.
- 13 G. Ferrer-Sueta and R. Radi, *ACS Chem. Biol.* 2009, **4**, 161.
- 14 R. Radi, *J. Biol. Chem.* 2013, **288**, 26464.
- 15 K. Abbas, M. Hardy, F. Poulhes, H. Karoui, P. Tordo, O. Ouari and F. Peyrot, *Free Rad. Biol. Med.* 2014, **71**, 281.
- 16 R. Chen, J. T. Warden and J. A. Stenken, *Anal. Chem.* 2004, **76**, 4734.
- 17 B. Gopalakrishnan, K. M. Nash, M. Velayutham and F. A. Villamena, *J. Visual. Exp.* 2012, E2810/1.
- 18 D. G. Mitchell, G. M. Rosen, M. Tseitlin, B. Symmes, S. S. Eaton and G. R. Eaton, *Biophys. J.* 2013, **105**, 338.
- 19 H. B. Hong, H. J. Krause, S. W. Sohn, T. K. Baik, J. H. Park, S. W. Shin, C. H. Park and D. Y. Song, *Anal. Biochem.* 2014, **447**, 141.
- 20 X. J. Chen, A. C. West, D. M. Crokek and S. Banta, *Anal. Chem.* 2008, **80**, 9622.
- 21 B. Derkus, E. Emregul and K. C. Emregul, *Talanta* 2015, **134**, 206.
- 22 H. Flamm, J. Kieninger, A. Weltin and G. A. Urban, *Biosen. Bioelectron.* 2015, **65**, 354.
- 23 M. Ganesana, J. S. Erlichman and S. Andreescu, *Free Rad. Biol. Med.* 2012, **53**, 2240.
- 24 G. Moschopoulou and S. Kintzios, *Anal. Chim. Acta* 2006, **573+574**, 90.
- 25 C. Lu, G. Song and J.-M. Lin, *TrAC, Trends Anal. Chem.* 2006, **25**, 985.
- 26 N. Soh, *Anal. Bioanal. Chem.* 2006, **386**, 532.
- 27 J. J. Gao, K. H. Xu, B. Tang, L. L. Yin, G. W. Yang and L. G. An, *FEBS J.* 2007, **274**, 1725.
- 28 N. Li, H. Wang, M. Xue, C. Chang, Z. Chen, L. Zhuo and B. Tang, *Chem. Commun.* 2012, **48**, 2507.
- 29 W. Zhang, P. Li, F. Yang, X. Hu, C. Sun, W. Zhang, D. Chen and B. Tang, *J. Am. Chem. Soc.* 2013, **135**, 14956.
- 30 B. Bekdeser, M. Ozyurek, K. Guclu and R. Apak, *Anal. Chem.* 2011, **83**, 5652.
- 31 D. Oushiki, H. Kojima, T. Terai, M. Arita, K. Hanaoka, Y. Urano and T. J. Nagano, *J. Am. Chem. Soc.* 2010, **132**, 2795.
- 32 J. Zielonka and B. Kalyanaraman, *Free Rad. Bio. Med.* 2010, **48**, 983.
- 33 K. M. Robinson, M. S. Janes, M. Pehar, J. S. Monette, M. F. Ross, T. M. Hagen, M. P. Murphy and J. S. Beckman, *Proc Natl. Acad. Sci. USA* 2006, **103**, 15038.
- 34 C. D. Georgiou, I. Papapostolou and K. Grintzalis, *Nat. Protocols* 2008, **3**, 1679.
- 35 I. Wang, S. Liu, Z. Zheng, Z. Pi, F. Song and Z. Liu, *Anal. Methods* 2015, **7**, 1535.
- 36 H. Maeda, K. Yamamoto, Y. Nomura, I. Kohno, L. Hafsi, N. Ueda, S. Yoshida, M. Fukuda, Y. Fukuyasu, Y. Yamauchi and N. Itoh, *J. Am. Chem. Soc.* 2005, **127**, 68.
- 37 H. Maeda, K. Yamamoto, I. Kohno, L. Hafsi, N. Itoh, S. Nakagawa, N. Kanagawa, K. Suzuki and T. Uno, *Chem. Eur. J.* 2007, **13**, 1946.
- 38 K. Xu, X. Liu, B. Tang, G. Yang, Y. Yang and L. G. An, *Chem. Eur. J.* 2007, **13**, 1411.
- 39 G. Manfredi, J. Fu, J. Ojaimi, J. E. Sadlock, J. Q. Kwong, J. Guy and E. A. Schon, *Nat. Genetics* 2002, **30**, 394.
- 40 Y. Chen, M. B. Azad and S. B. Gibson, *Cell Death Differentiation* 2009, **16**, 1040.
- 41 P. Huang, L. Feng, E. A. Oldham, M. J. Keating and W. Plunkett, *Nature* 2000, **407**, 390.
- 42 H. Zheng, X.-Q. Zhan, Q.-N. Bian and X.-J. Zhang, *Chem. Comm.* 2013, **49**, 429.
- 43 R. Sjoback, J. Nygren, and M. Kubista, *Spectrochim. Acta A.* 1995, **51**, L7-L21.
- 44 N. Demaurex, *News Physiol. Sci.*, 2002, **17**, 1-5.
- 45 J. Llopis, J. M. McCaffery, A. Miyawaki, M. G. Farquhar, and R. Y. Tsien, *Proc. Natl. Acad. Sci. USA*, 1998, **95**, 6803-6808.
- 46 B. C. Dickinson, C. Huynh and C. J. Chang, *J. Am. Chem. Soc.* 2010, **132**, 5906.

Table of Entry

A fluorogenic probe with mitochondria targeting capability was prepared for detection of superoxide radical generation inside mitochondria in living cells.

